

## **MICROBALANCE TECHNIQUES IN DESIGN AND CONTROL OF SYNTHETIC CARBONS**

*A. M. Puziy\* and O. I. Poddubnaya*

Institute for Sorption and Problems of Endoecology, National Academy of Sciences of Ukraine  
Naumov St. 13, 252164 Kyiv, Ukraine

### **Abstract**

Peculiarities of carbonization of two styrene/divinylbenzene precursors (one sulfonated, another aminated and phosphorylated) have been investigated by thermogravimetry and differential thermal analysis. It was shown that phosphorus compounds incorporate into carbon structure and cause delayed carbonization. Porous structure and surface properties of synthetic carbons have been investigated by standard (BET,  $\alpha_s$  method, DA) and advanced (AED, PSD, regularization) methods from benzene and water adsorption isotherms. It was shown that phosphorus-containing carbon is less microporous and shows highly hydrophilic surface.

**Keywords:** adsorption, adsorption energy distribution, carbonization of polymers, pore size distribution, porosity, thermogravimetric analysis

### **Introduction**

Microbalance techniques are widely used for design and control of porosity and surface properties of carbon adsorbents. Thermogravimetric analysis (TG) shows the progress of pyrolysis of polymer precursors and thus allows optimization of carbonization process for obtaining adsorbent with enhanced performance. Gas adsorption (vacuum microbalance technique) appears to be the most suitable characterization method, since it allows to obtain information about both porosity and surface characteristics of the materials depending on the adsorbate nature.

In the present paper TG is used for the investigation of pyrolysis process and gas adsorption (vacuum microbalance technique) is applied for the characterisation of porous structure and surface properties of two types of synthetic carbons obtained from two different styrene/divinylbenzene co-polymers.

### **Experimental**

Two styrene/divinylbenzene polymer precursors were used in the present study. First, the polymer precursor of synthetic carbon SCS was obtained by chloromethylation

\* Author for correspondence: E-mail: alexander.puziy@ispe.kiev.ua

and sulfonation of styrene/divinylbenzene copolymer [1, 2]. This polymer precursor contains  $-\text{COOH}$  and  $-\text{SO}_3\text{H}$  functional groups. Second, the polymer precursor of NPC carbon was obtained by chloromethylation, amination and phosphorylation of styrene/divinylbenzene copolymer [3–5]. This polymer precursor contains functional  $=\text{N}-$  and  $-\text{N}=\text{P}(\text{OH})=$  groups.

TG was performed by using Derivatograph Q-1500 (MOM, Hungary) in argon atmosphere with a heating rate of  $10^\circ\text{C min}^{-1}$ .

Adsorption isotherms of benzene and water were determined at  $20^\circ\text{C}$  by using a vacuum gravimetric adsorption system consisting of quartz springs with a constant approximately  $0.15\text{--}0.30 \text{ mm mg}^{-1}$ ; the spring extension was measured with a cathetometer to a precision of 0.01 mm. The sample was outgassed overnight under high vacuum at  $250^\circ\text{C}$ .

## Results and discussion

When a polymer matrix is exposed to high temperatures the energy is transferred from surrounding area to the polymer matrix, resulting in a series of chemical reactions which transform polymer precursor to a carbon residue. Pyrolysis proceeds by a combination of two competing processes, chain scission to volatile carbon compounds and chain condensation to carbon-like residues. Polymer degradation results in volatile generation and mass loss while chain condensation leads to carbon residue, which is essential to carbon adsorbent manufacture.

Pyrolysis of the polymer precursors was investigated using TG (Fig. 1). DTG traces of both precursors are similar and show two distinct peaks with increased rate of mass loss. The first peak is obviously associated with the evaporation of water. The second peak corresponds to the most intensive degradation processes. It is interesting to note that this peak is  $50^\circ\text{C}$  higher for phosphorus-containing NPC polymer precursor-

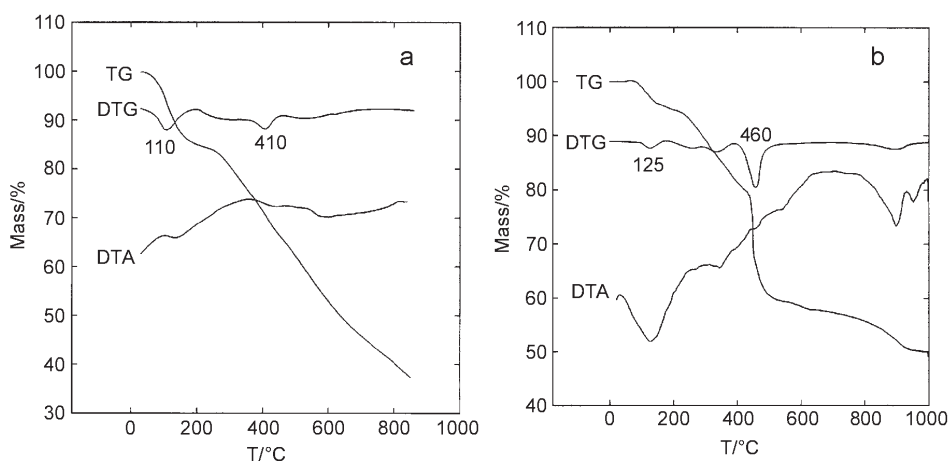


**Fig. 1** Thermogravimetric analysis a – of SCS and b – NPC precursors

sor than for SCS-precursor. This delayed carbonization is obviously due to the known fire-retardant effect of phosphorous compounds [6]. The yield of carbonaceous residue is 10% higher for phosphorus-containing copolymer, suggesting that phosphorus incorporates into carbon structure giving unique surface properties.

The adsorption isotherm of benzene at 25°C is shown in Fig. 2. The isotherms belong to type IV of IUPAC classification [7]. The initial part of the isotherm is attributed to monolayer-multilayer adsorption and hysteresis loop is associated with capillary condensation taking place in mesopores. A substantial part of the isotherm for SCS carbon is attributed to the micropore filling process, while isotherm for NPC

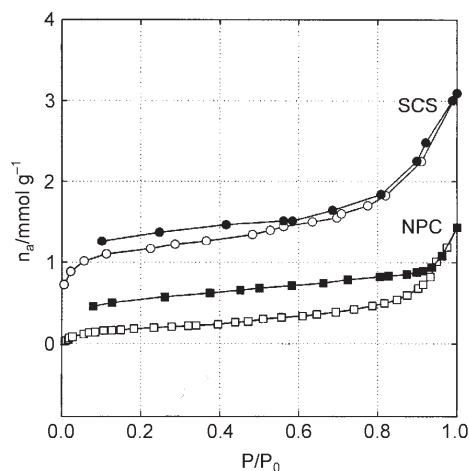


Fig. 2 Benzene adsorption (○□) and desorption (●■) isotherms on carbons SCS and NPC at 298 K

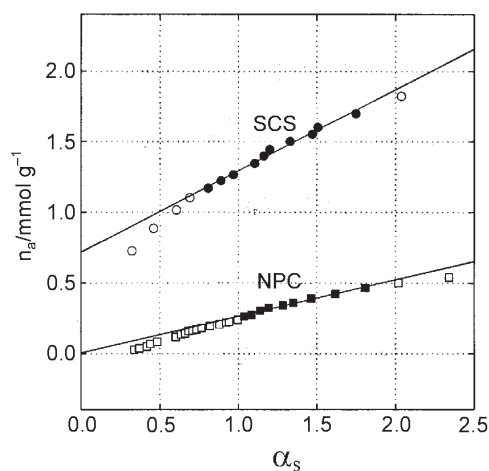
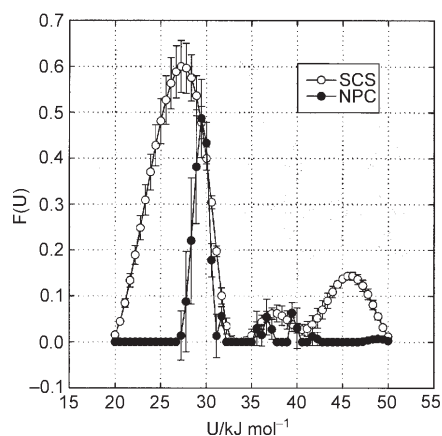


Fig. 3  $\alpha_s$  plot for carbons SCS and NPC

carbon resembles those on a non-porous adsorbent. At  $P/P_0=1$  micropores and mesopores completely filled with adsorbate. Thus, the amount adsorbed at this pressure, expressed by volume of liquid adsorbed, represents sorption pore volume of the adsorbent. For NPC the value of sorption pore volume is only  $0.12 \text{ cm}^3 \text{ g}^{-1}$  while for carbon SCS this value is more than two times larger –  $0.28 \text{ cm}^3 \text{ g}^{-1}$ . It is interesting, that the weak developed porous structure is characteristic of the non-activated synthetic carbons obtained by carbonization in inert atmosphere [1–9].

The  $\alpha_s$  plot for benzene adsorption isotherm is given in Fig. 3. There is a steep rise at low  $\alpha_s$  values for SCS carbon attributed to micropore filling. In contrast,  $\alpha_s$  plot for NPC carbon is linear over the 0–2 range of  $\alpha_s$  values showing non-porous character of this carbon. The  $\alpha_s$  plots for both carbons bend downward above  $\alpha_s=2.0$  as for other activated carbons [10]. The bending at high values of  $\alpha_s$  is clearly associated with the presence of mesopores. The micropore volume estimated by linear extrapolation of the  $\alpha_s=1.0$ – $2.0$  region to  $\alpha_s=0$  is  $0.06 \text{ cm}^3 \text{ g}^{-1}$  for SCS carbon is negligibly small ( $0.0004 \text{ cm}^3 \text{ g}^{-1}$ ) for NPC carbon. Non-microporous (mesopore+macropore) surface area estimated from the slope of  $\alpha_s$ -plot is two times higher for SCS carbon ( $92 \text{ m}^2 \text{ g}^{-1}$ ) than for NPC carbon ( $41 \text{ m}^2 \text{ g}^{-1}$ ). Additional evidence for non-microporous character of NPC carbon is the similarity in BET surface area ( $212$  for SCS and  $38 \text{ m}^2 \text{ g}^{-1}$  for NPC) and  $\alpha_s$  surface area. As the NPC carbon is mesoporous, it may be concluded that phosphorus compounds in polymer precursor do not act as activating agent during pyrolysis as opposed to the phosphoric acid [11–16]. A total absence of microporosity in NPC may also be explained by the deposition of pyrolytic carbon from carbon-containing volatile products at high-temperature. The decreasing of microporosity upon heat treatment of active carbon in hydrocarbon atmosphere is known from the literature [17, 18].

Details of interaction of adsorbent surface with adsorbate molecule may be obtained from adsorption energy distribution. Figure 4 shows adsorption energy distributions for carbon SCS and NPC obtained by regularization method using localized adsorption



**Fig. 4** Adsorption energy distribution according to FFG model from benzene adsorption data for carbons SCS and NPC

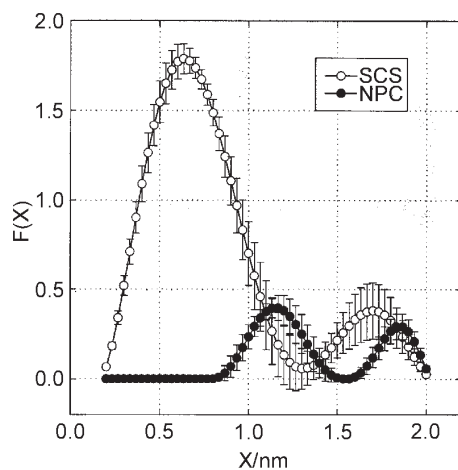


Fig. 5 Pore size distribution according to DA model for carbons SCS and NPC

model of Frumkin–Fowler–Guggenheim (FFG) [19]. High energy peaks ( $U > 35 \text{ kJ mol}^{-1}$ ) correspond to carbon–benzene interaction with flat surface ( $37\text{--}38 \text{ kJ mol}^{-1}$ ) and adsorption in micropores ( $46 \text{ kJ mol}^{-1}$ ) with enhanced potential, while the low energy peak is due to multilayer adsorption. It should be noted that carbon NPC does not show any peak in high energy region corresponding to benzene adsorption in micropores.

Once energy distribution is obtained, one can calculate pore size distribution function provided that relationship between energy and pore size is known. Figure 5 shows pore size distribution according to Dubinin–Astakhov (DA) model with exponent equal 3 and energy–size relationship  $X=k/E$ ,  $k=12 \text{ kJ mol}^{-1} \text{ nm}$  [20]. It is seen

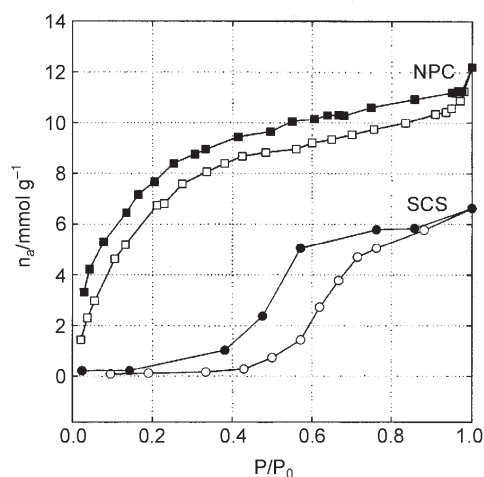
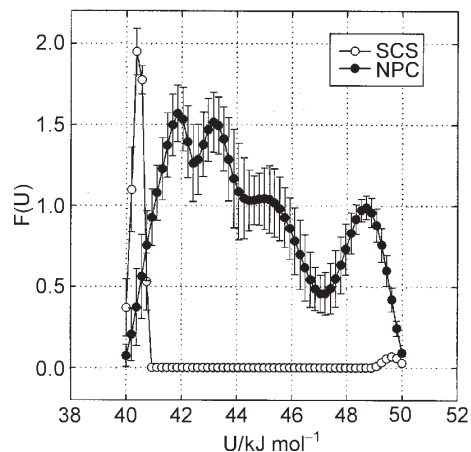


Fig. 6 Water adsorption (o□) and desorption (●■) isotherms on carbons SCS and NPC at 298 K



**Fig. 7** Adsorption energy distribution according to FFG model from water adsorption data for carbons SCS and NPC

from this figure that there is no any peak for NPC carbon at micropore region ( $X < 1$  nm) while carbon SCS shows considerable amount of micropores.

It is well known that the exact shape of the water isotherm is highly dependent on the surface properties of carbon. Purely carbonaceous adsorbents show weak interaction with water molecules and thus adsorption isotherm belongs to type III of IUPAC classification [7]. However, this hydrophobic character may be changed by introducing various heteroatoms in carbon structure, like O, N, etc. Water adsorption isotherms are shown in Fig. 6. The difference between carbons is obvious: water adsorption on SCS carbon is of type III showing hydrophobic surface, while NPC carbon shows isotherm of type IV showing strongly hydrophilic surface. This effect is due to phosphorus heteroatoms in carbon structure.

Figure 7 shows details of distribution of hydrophilic sites obtained by the regularization method using FFG model from water adsorption data. SCS carbon shows a very small peak at  $49 \text{ kJ mol}^{-1}$  corresponding to oxygen-containing surface groups and one low energy peak corresponding to micropore filling with water. The distribution for NPC carbon is completely different and shows multiple peaks with maximum at  $42, 43, 45$  and  $49 \text{ kJ mol}^{-1}$ .

## Conclusions

TG was used for analysis of pyrolysis of two polymer precursors and vacuum microbalance technique is used for adsorption measurements on SCS and NPC carbons. It was shown that phosphorus compounds cause delayed carbonization. Phosphorus compounds incorporates into carbon structure during carbonization and confer hydrophilic properties to carbon adsorbent.

## References

- 1 A. M. Puziy, *Langmuir*, 11 (1995) 543.
- 2 N. T. Kartel and A. M. Puziy, *The European Conference Carbon 96*, Newcastle, UK 1996, p. 525.
- 3 A. M. Puziy and O. I. Poddubnaya, *Carbon*, 36 (1998) 45.
- 4 B. N. Laskorin, N. G. Zhukova and O. P. Polyakova, *Proizvodstvo i Pererabotka Plastmass i Sinteticheskikh Smol*, N8 (1977) 3.
- 5 *Ion Exchange Materials for Hydrometallurgy, Waste Water and Water Treatment*, VNIINTI, Moscow 1982 (in Russian).
- 6 M. Le Bras, S. Bourbigot, Y. Le Tallec and J. Laureyns, *Polymer Degradation and Stability*, 56 (1997) 11.
- 7 K. S. W. Sing, D. H. Everett, R. A. W. Haul, L. Moscou, R. A. Pierotti, J. Rouquérol and T. Siemieniowska, *Pure and Appl. Chem.*, 57 (1985) 603.
- 8 J. Choma, M. Jaroniec and A. M. Puziy, *Karbo-Energochemia-Ecologia*, (1993) 237.
- 9 A. M. Puziy, R. Leboda, V. I. Bogillo, V. P. Shkilev and A. Lodyga, *Ads. Sci. Techn.*, 12 (1995) 267.
- 10 N. Setoyama, K. Kaneko and F. Rodriguez-Reinoso, *J. Phys. Chem.*, 100 (1996) 10331.
- 11 J. Laine, A. Calafat and M. Labady, *Carbon*, 27 (1989) 191.
- 12 J. Laine and S. Yunes, *Carbon*, 30 (1992) 601.
- 13 M. Yagtoyen, M. Thwaites, J. Stencil, B. McEnaney and F. Derbyshire, *Carbon*, 30 (1992) 1089.
- 14 M. Molina-Sabio, F. Rodriguez-Reinoso, F. Caturla and M. J. Sellés, *Carbon*, 33 (1995) 1105.
- 15 M. Molina-Sabio, F. Caturla and F. Rodriguez-Reinoso, *Carbon*, 33 (1995) 1180.
- 16 M. Molina-Sabio, F. Rodriguez-Reinoso, F. Caturla and M. J. Sellés, *Carbon*, 34 (1996) 457.
- 17 Y. Kawabuchi, S. Kawano and I. Mochida, *Carbon*, 34 (1996) 711.
- 18 Y. Kawabuchi, M. Kishino, S. Kawano, D. D. Whitehurst and I. Mochida, *The European Conference Carbon 96*, Newcastle, UK 1996, p. 570.
- 19 A. M. Puziy, T. Matynya, B. Gawdzik and O. I. Poddubnaya, *Langmuir*, 15 (1999) 6016.
- 20 A. M. Puziy, V. V. Volkov, O. I. Poznayeva, V. I. Bogillo and V. P. Shkilev, *Langmuir*, 13 (1997) 1303.